Molecular Therapy
Original Article

miR-23b Suppresses Leukocyte Migration and Pathogenesis of Experimental Autoimmune Encephalomyelitis by Targeting CCL7

Yuan Zhang,[1,2,3] Juan-Juan Han,[1,3] Xiao-Yan Liang,[1,3] Li Zhao,[1] Fei Zhang,[1] Javad Rasouli,[2] Zhe-Zhi Wang,[1] Guang-Xian Zhang,[2] and Xing Li[1,2]

[1]Key Laboratory of the Ministry of Education for Medicinal Resources and Natural Pharmaceutical Chemistry, National Engineering Laboratory for Resource Development of Endangered Crude Drugs in Northwest China, College of Life Sciences, Shaanxi Normal University, Xi'an 710119, China; [2]Department of Neurology, Thomas Jefferson University, Philadelphia, PA 19107, USA

MicroRNAs (miRNAs) are small, non-coding RNAs involved in immune response regulation. Specific miRNAs have been linked to the development of various autoimmune diseases; however, their contribution to the modulation of CNS-directed cellular infiltration remains unclear. In this study, we found that miR-23b, in addition to its reported functions in the suppression of IL-17-associated autoimmune inflammation, halted the progression of experimental autoimmune encephalomyelitis (EAE), an animal model of multiple sclerosis (MS), by directly inhibiting the migration of pathogenic leukocytes to the CNS. We demonstrated that miR-23b was specifically decreased during the acute phase of EAE and that overexpression of miR-23b resulted in a defect in leukocyte migration and strong resistance to EAE. Furthermore, we found that miR-23b suppressed leukocyte migration of EAE by targeting CCL7, a chemokine that attracts monocytes during inflammation and metastasis. Finally, in the adoptive transfer model, miR-23b reduced the severity of EAE by inhibiting the migration of pathogenic T cells to the CNS rather than diminishing the encephalitogenesis of T cells. Taken together, our results characterize a novel aspect of miR-23b function in leukocyte migration, and they identify miR-23b as a potential therapeutic target in the amelioration of MS and likely other autoimmune diseases.

INTRODUCTION

Multiple sclerosis (MS) is a chronic inflammatory demyelinating disease resulting from an autoimmune response against CNS myelin.[1] Abnormal inflammatory responses, initialized by autoreactive $CD4^+$ T cells, promote tissue damage of the CNS in MS and its animal model, experimental autoimmune encephalomyelitis (EAE).[2] Among these $CD4^+$ T cells, Th1 cells that produce interferon-γ (IFN-γ) and Th17 cells that secrete IL-17, IL-22, and granulocyte-macrophage colony-stimulating factors (GM-CSFs) are the major encephalitogenic cells that, upon entering the CNS, activate microglia and astrocytes to produce large numbers of cytokines and chemokines, which further recruit peripheral immune cells to the site of inflammation.[3–5] A therapeutic strategy that focuses on modulation of the immune response and pathogenic T cell infiltration in the CNS would improve treatment efficacy.

MicroRNAs (miRNAs) are a class of evolutionarily conserved, short endogenous non-coding RNAs that regulate gene expression at the post-transcriptional level.[6] They bind to the 3′ UTR of the target mRNAs and lead to the degradation or translational inhibition of the target mRNAs.[7] miRNAs play critical roles in multiple biological processes, such as the regulation of immune cell differentiation and correction of CNS functioning, and they are thus novel tools for diagnosis and therapy for several diseases.[8] The involvement of miRNAs has been reported in the pathogenesis of autoimmune diseases such as systemic lupus erythematosus, rheumatoid arthritis, type I diabetes, and asthma.[6,9–12] Aberrant expression of miRNAs has also been linked to MS and other inflammatory diseases.[13,14] For instance, miR-20b has been found to negatively regulate Th17 differentiation by targeting RORγt and STAT3, and its expression was significantly downregulated in blood cells of MS patients as compared with healthy controls.[15] Mice lacking miR-155 showed reduced CNS inflammation, and anti-miR-155 treatment ameliorated EAE disease severity.[16,17] miR-let-7e has been found to play an important role in Th1 and Th17 development, and inhibiting its expression shifted the immune response to a Th2 profile, halting disease progression of EAE.[7] miR-326 is among the most upregulated miRNAs in active MS lesions and blood compared with control specimens; deletion of miR-326 significantly halted disease development.[18] Further, miR-301 has been shown to regulate Th17-mediated immune responses by targeting the IL-6/23-STAT3 pathway, and EAE severity was obviously altered by modulating miR-301a levels.[19] These reports

Received 16 June 2017; accepted 22 November 2017;
https://doi.org/10.1016/j.ymthe.2017.11.013.

[3]These authors contributed equally to this work.

Correspondence: Guang-Xian Zhang, Thomas Jefferson University, Department of Neurology, Philadelphia, PA 19107, USA.
E-mail: guang-xian.zhang@jefferson.edu
Correspondence: Xing Li, Shaanxi Normal University, College of Life Sciences, No. 620, West Chang'an Avenue, Xi'an 710119, China.
E-mail: xingli_xian@126.com

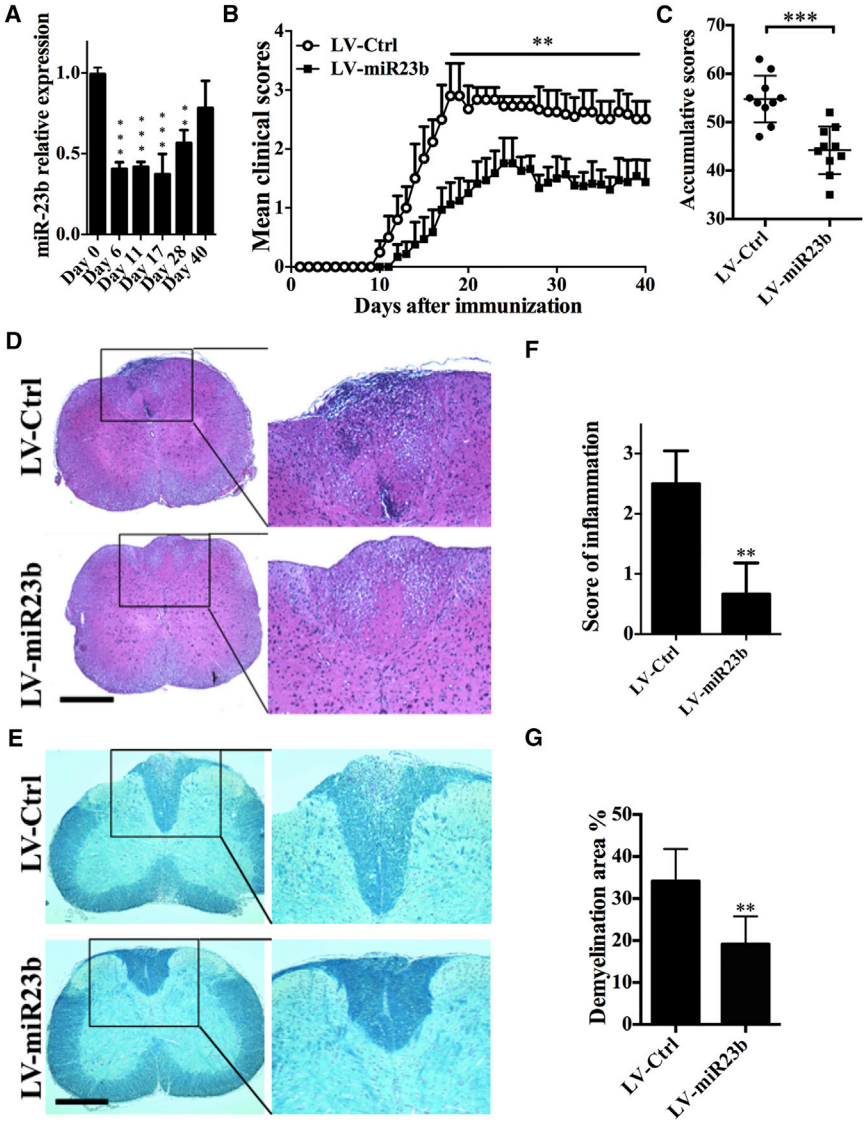

Figure 1. i.v. Injection of miR-23b Lentivirus Ameliorates Disease Severity

(A) RT-PCR detection of spinal cord miR-23b level in C57BL/6 mice after active immunization. (B) C57BL/6 mice were injected intravenously with 2×10^7 IU/mouse lentivirus 5 days before MOG_{35-55} immunization. (C) Cumulative clinical score of each mouse was calculated by summing up the scores of the mouse from day 0 to day 40 p.i. (D and E) Histological examination of inflammatory lesions and demyelination in the lumbar spinal cord of LV-Ctrl- or LV-miR23b-treated mice by (D) H&E staining and (E) Luxol fast blue staining (scale bar, 1 mm) at day 40 p.i. (F and G) Statistical analysis of (D) is in (F) and (E) is in (G). Data represent three independent experiments. Data are mean ± SD (n = 10 each group). **p < 0.01 and ***p < 0.001, determined by one-way ANOVA (A), unpaired Student's t test (B, C, and G), or nonparametric test (F).

provide evidence of a relationship between miRNA and MS/EAE; however, the potential role of miRNAs in the context of MS/EAE is still unclear.

miR-23b has been identified as a commonly downregulated miRNA in patients with autoimmune diseases such as rheumatoid arthritis; systemic lupus erythematosus; and in mouse models of collagen-induced arthritis (CIA), MRL/lpr, and EAE. In addition, miR-23b suppresses the pathogenesis of multiple autoimmune diseases by targeting proinflammatory cytokine-mediated signaling.[19] Despite these reported functions of miR-23b in antigen- specific inflammatory responses against self-tissues, to date there has been little evidence that endogenously expressed miR-23b impacts leukocyte migration *in vivo*.

In this study, we characterize a previously unknown miR-23b function in leukocyte migration, and we identify miR-23b as a potential therapeutic target in the amelioration of MS and other autoimmune diseases.

RESULTS

Expression of miR-23b in the CNS after EAE Induction

To study the role of miR-23b in EAE development, we first sought to analyze miR-23b expression in mice during the course of EAE. Thus, the CNS was harvested from mice with EAE at different time points after disease induction, and the expression level of miR-23b was analyzed by real-time PCR. We found that miR-23b expression in the CNS was significantly decreased during the acute phase, when CNS tissues were assayed on days 6, 11, 17, and 28 post-immunization (p.i.), and this expression returned to normal at the chronic stage, e.g., day 40 p.i. (Figure 1A). These results indicated an important role of miR-23b expression in the disease priming stage during EAE progression.

Overexpression of miR-23b Resulted in the Inhibition of EAE and the Reduction of CNS Inflammation

To determine whether miR-23b expression can influence the development of EAE, we developed the lentivirus vectors that can, *in vivo*, increase expression levels of miR-23b (labeled as LV-miR23b), and a mutant miR-23b served as the negative control (labeled as LV-Ctrl). We introduced 2×10^7 transforming unit recombinant lentivirus into mice by intravenous (i.v.) injection. Similar with previous studies,[15,18] no significant difference in miR-23b expression level was found in heart, lung, or heart after lentivirus injection, while approximately 1.5- to 2.5-fold induction was found in spleen, lymph nodes, and brain (Figure S1). On day 5 post-virus delivery, mice were immunized with myelin

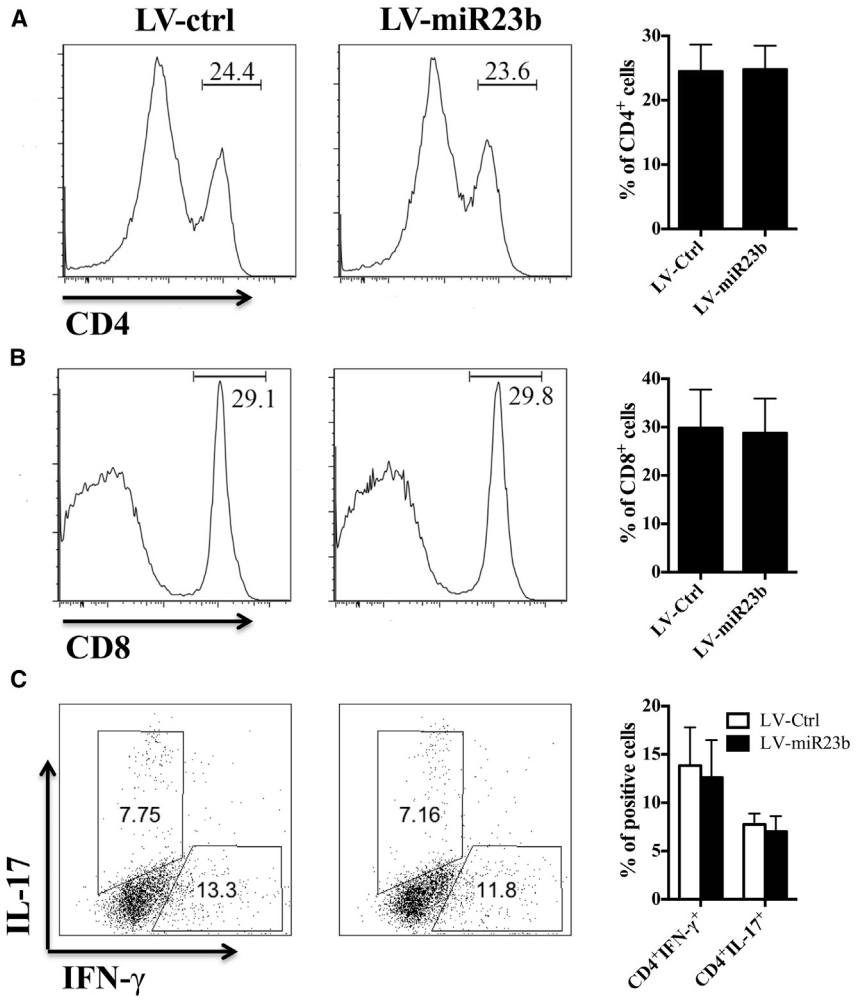

Figure 2. LV-miR23b Does Not Suppress T Cell Activation in the Periphery

(A and B) Flow cytometry analysis of (A) $CD4^+$ and (B) $CD8^+$ T cell population in splenocytes from LV-Ctrl- and LV-miR23b-treated mice at day 10 p.i. (disease onset). (C) Flow cytometry analysis of the percentage of IFN-γ or IL-17 produced by Th1 or Th17 cells in splenocytes. Data are mean ± SD (n = 5 each group; unpaired Student's t test).

oligodendrocyte glycoprotein peptide (MOG_{35-55}). LV-Ctrl-treated mice with severe disease signs, such as limping and tail and limb paralysis, were observed with a maximum EAE score at day 17 p.i. (maximum EAE score, 2.9 ± 0.55). LV-miR23b-treated mice showed less severe disease (maximum EAE score, 1.6 ± 0.22) (Figure 1B), accompanied by a reduced accumulative score (Figure 1C). Furthermore, disease onset was delayed in LV-miR23b-treated mice as compared with LV-Ctrl-treated mice (day 13 versus day 11 p.i.). Taken together, these findings indicate that miR-23b plays a critical role in EAE development.

Consistent with the clinical score, histological examination of the spinal cords of LV-Ctrl-treated and LV-miR23b-treated mice revealed a significant difference. LV-Ctrl-treated mice displayed the characteristic EAE histological alteration, including massive parenchymal lymphocytic infiltration, perivascular cuffing with mononuclear cells, and demyelination in lumbar spinal cord (Figures 1D–1G). In contrast, inflammatory cells infiltrated into the CNS through subpial and perivascular region were minimally detected in the spinal cords of LV-miR23b-treated mice (Figures 1D and 1E). Furthermore, LV-miR23b-treated mice showed less demyelination than LV-Ctrl-treated mice (Figures 1F and 1G).

Disease Amelioration in LV-miR23b-Treated EAE Mice Does Not Impair Subpopulations of Encephalitogenic T Cells in the Periphery

After immunization, antigen-specific T cells were primed in the periphery before migration into the CNS.[20] To evaluate the possibility of a potential immunomodulatory profile of miR-23b, we tested the MOG-specific T cell populations in secondary lymphoid organs of LV-miR23b- and LV-Ctrl-treated EAE mice at disease onset (day 10 p.i.). Results showed that overexpression of miR-23b did not change the percentages of MOG-specific $CD4^+$ and $CD8^+$ T cells in spleen (Figures 2A and 2B) at disease onset or the intracellular productions of IL-17 and IFN-γ by Th17 and Th1 cells (Figure 2C). These results indicate that the therapeutic effect of miR-23b on EAE is not due to impaired T cell responses in the periphery.

Overexpression of miR-23b Impaired CNS-Directed Encephalitogenic T Cell Infiltration

After priming in the periphery, encephalitogenic leukocytes infiltrate into CNS parenchyma for a second wave of damage.[21] As miR-23b did not impair lymphocyte activation in the periphery, this suggested that the mechanism of action exerted by miR-23b is dependent on the inhibition of CNS-directed lymphocyte trafficking rather than modulation of the immune response. To test this hypothesis, we tested the frequency as well as absolute number of leukocyte subpopulations that infiltrated in the CNS between these groups. Compared with the LV-Ctrl-treated group, disease amelioration correlated closely with a reduction in the infiltration of $CD45^+$ leukocytes in the CNS of LV-miR23b-treated EAE mice (Figures 3A and 3B). In addition, mononuclear cells (MNCs) were isolated from the CNS and analyzed by flow cytometry. The total number of MNCs was 236.6 ± 18.67 × 10^4 per mouse in the LV-Ctrl-treated group versus 124.7 ± 17.02 × 10^4 per mouse in the LV-miR23b-treated group (Figure 3C).

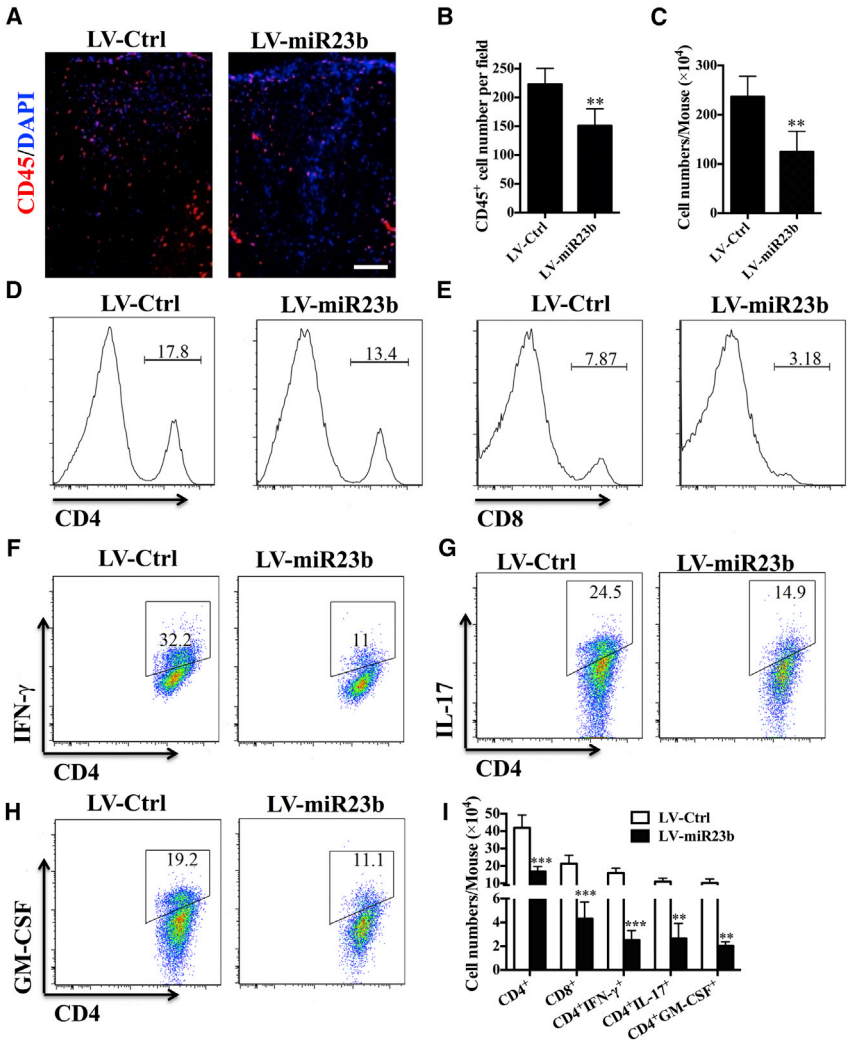

Figure 3. LV-miR23b Limits CNS-Directed T Lymphocyte Extravasation

(A) Immunohistochemistry staining of $CD45^+$ cells in spinal cord of LV-Ctrl- and LV-miR23b-treated mice (day 17 p.i.). (B) Statistical analysis of (A). (C) Spinal cords and brains were harvested and MNCs isolated (n = 5 each group). Total MNC numbers in the CNS were counted under light microscopy. (D–H) Percentages of (D) $CD4^+$ and (E) $CD8^+$ T cells among MNCs and (F) IFN-γ^+, (G) IL-17^+, and (H) GM-CSF^+ cells among $CD4^+$ T cells were determined by flow cytometry. (I) Absolute numbers of different subtypes of CNS-infiltrating cells were calculated by multiplying the percentages of these cells by total numbers of MNCs obtained from each spinal cord of mice. Data are mean ± SD (n = 5 each group). **p < 0.01 and ***p < 0.001, determined by one-way ANOVA (A) or unpaired Student's t test.

Flow cytometry analysis demonstrated that LV-miR23b-treated mice presented a lower frequency and numbers of $CD4^+$ and $CD8^+$ cells in spinal cord (Figures 3D, 3E, and 3I). Of note, significantly fewer infiltrations of $CD4^+$IFN-γ^+, $CD4^+$IL17^+, and $CD4^+$GM-CSF^+ cells in the CNS of LV-miR23b-treated-mice were observed (Figures 3F–3I). These results indicated that miR-23b reduced recruitment and infiltration into the CNS of pathological $CD4^+$ T cells, specifically Th1 and Th17 cells.[5] That is to say, disease amelioration in miR-23b-treated mice depends on the inhibition of encephalitogenic T cell migration.

CCL7 Is the Functional Target of miR-23b

To identify potential targets of miR-23b, we used TargetScan to look for gene transcripts downregulated by miR-23b overexpression. We found that a secreted chemokine gene, CCL7, has a putative binding site in the 3′ UTR of miR-23b (Figure 4A). We then analyzed gene expression of chemokine receptors in draining lymph nodes (dLNs) at disease onset (day 10 p.i.) and chemokine ligands in the CNS at the peak of disease severity (day 17 p.i.). Results showed that, among all the tested chemokine receptors and ligands, only CCL7 expression was significantly decreased in the dLNs and CNS of LV-miR23b-treated mice (Figures 4B and 4C) compared to LV-Ctrl-treated mice, indicating that miR-23b plays a critical role in the regulation of CCL7 production. Consistent with the qPCR results, the protein level of CCL7 in CNS homogenates, as measured by western blot, was significantly decreased in mice treated with LV-miR23b compared to those treated with LV-Ctrl (Figures 4D and 4E).

To further corroborate that miR-23b could specifically and directly bind to CCL7, we constructed a dual-direction fluorescence reporter (mCherry and copGFP) vector (Figure 4F) to test the prediction by TargetScan. The 3′ UTR of CCL7 was ligated after mCherry and copGFP was inserted as an internal control. These two reporter genes were controlled by a dual-directional promoter. Among the GFP^+ cells, we observed remarkably decreased numbers of $GFP^+$$mCherry^+$ cells and a decrease in mCherry fluorescence intensity by transfection of miR-23b mimics, compared with mutant miR-23b mimics (Figures 4G and 4H).

Astrocytes are the source of CCL7 in the CNS.[22] To assess the mRNA level of CCL7 in astrocytes of LV-miR23b-treated mice, astrocytes were isolated using anti-ACSA-2 microbeads, after which the GFP^+ (lentivirus-infected) astrocytes were sorted by fluorescence-activated cell sorting (FACS), with a purity of >95% GFP^+ (Figure S2; Figure 4I). Consistently, genes of the astrocyte-related markers gfap, aqp4, and aldh111 were highly expressed in sorted astrocyte fraction (ACSA-2+; Figure S3). Further, the CCL7 expression level in GFP^+ astrocytes from LV-miR23b-treated mice was significantly downregulated compared with those from LV-Ctrl-treated mice (Figure 4J),

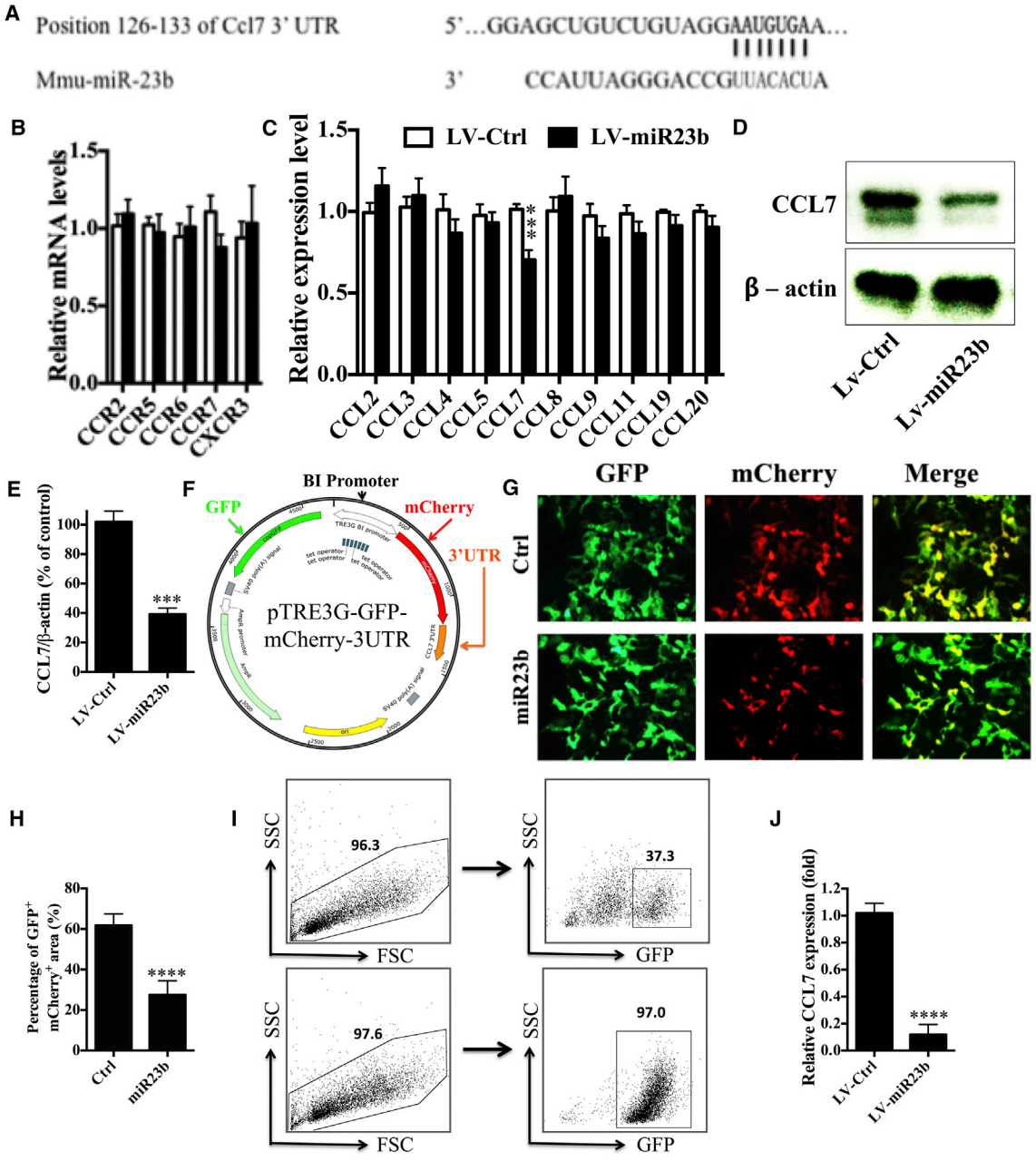

Figure 4. CCL7 Is the Functional Target of miR-23b

(A) Matched sequence of CCL7 3′ UTR-binding site. (B) Draining lymph nodes were collected from EAE mice at day 10 p.i. (C) CNS was collected at day 17 p.i. Tissues were submitted to RNA extraction and cDNA production. Analysis of expression of genes of interest was carried out by RT-PCR. (D) EAE mice treated with LV-miR23b or LV-Ctrl were sacrificed at day 17 p.i. Brain and spinal cord tissues were harvested and homogenized for western blot. (E) Densitometry was determined by ImageJ and data were analyzed by Graphpad Prism. (F) Schematic of bi-directional fluorescence reporter vector. (G) HEK293 cells were transfected with pDual-GFP/mCherry-CCL7 3′ UTR 3 days before transfection with miR-23b mimic or control mimic, as described in the Materials and Methods. After 24 hr, cells were checked under fluorescence microscopy. (H) Statistical analysis of (G) by Image-Pro Plus software. (I) Sorting GFP-positive cells by FACSAria. Flow cytometry analysis of GFP$^+$ cell population before (upper level) and post-sorting (lower level) is shown. (J) CCL7 expression level was performed by qPCR. Data are mean ± SD (n = 5 each group) and analyzed by unpaired Student's t test (**p < 0.01, ***p < 0.001, and ****p < 0.0001).

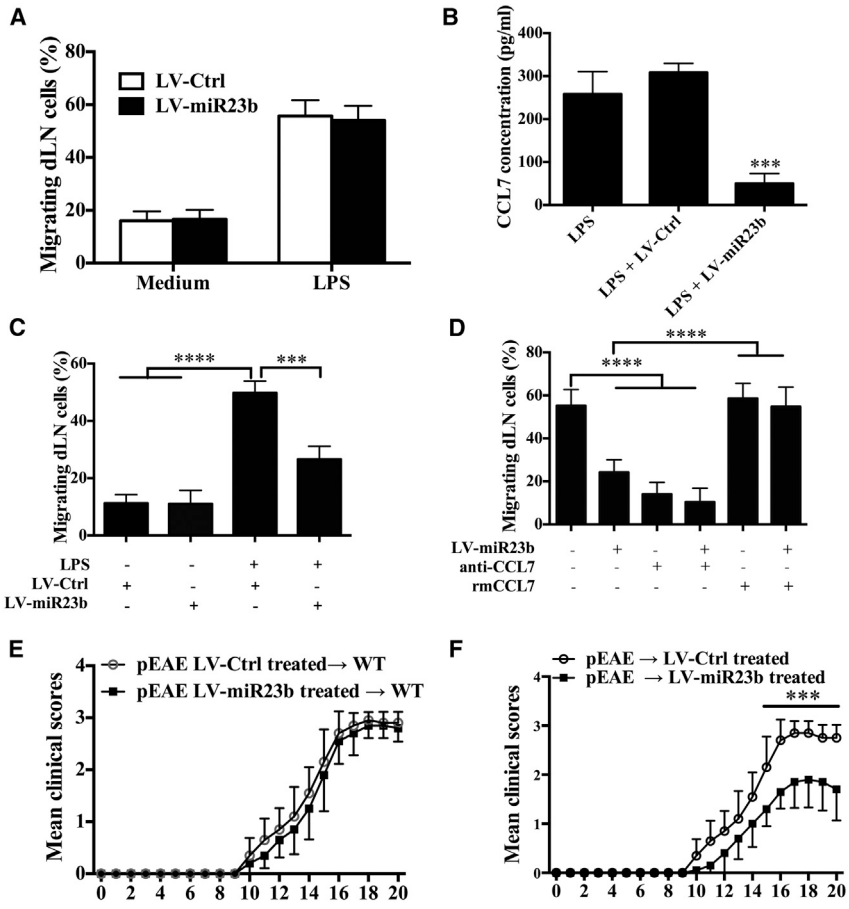

Figure 5. LV-miR23b Reduces Cell Migration

(A) C57BL/6 mice were injected intravenously with lentivirus 5 days before MOG_{35-55} immunization. At 10 days p.i., mice were sacrificed and draining lymph nodes were collected. Single-cell suspensions (5×10^5 cells) were prepared and seeded on the upper level of transwell plates. The lower chamber was seeded with astrocytes that had been activated by LPS 24 hr before. Cells were incubated for 3 hr at 37°C. At the end of culture time, cells in the lower chamber were counted by hemocytometer. (B) Astrocytes were isolated and infected with LV-Ctrl or LV-miR23b for 3 days. Then after being activated by LPS for 24 hr, supernatants were harvested and CCL7 concentrations were determined by ELISA kits. (C) At 10 days p.i., EAE mice were sacrificed and cells of draining lymph nodes were seeded on the upper level of transwell plates. In the lower chamber, astrocytes activated by LPS were added with LV-Ctrl or LV-miR23b. Lower level cells were counted after 3-hr culture. (D) Astrocytes were infected with LV-miR23b; 3 days later, cells were incubated with LPS and anti-CCL7 (50 ng/mL) or murine recombinant CCL7 (1 ng/mL). Draining lymph nodes were seeded on the upper level of transwell plates, and the numbers of migrated cells were counted after 3-hr culture. (E) Spleen and draining lymph nodes from LV-Ctrl- or LV-miR23b-treated EAE mice at day 10 p.i. were collected, and MNCs were cultured with MOG_{35-55} + IL-23 + IL-2 for 3 days. Cells were intravenously injected into naive mice, and the clinical course of passive EAE (pEAE) mice was evaluated daily. (F) Spleen and draining lymph nodes from EAE mice at day 10 p.i. were collected and cultured with MOG_{35-55} + IL-23 + IL-2 for 3 days. Cells were intravenously injected into naive mice that had been treated with LV-Ctrl or LV-miR23b 5 days previously. Clinical course of passive EAE mice was evaluated daily. Data are mean ± SD (n = 10 each group; unpaired Student's t test, $^{**}p < 0.01$, $^{***}p < 0.001$, and $^{****}p < 0.0001$).

indicating the efficient suppression of CCL7 expression by miR-23b *in vivo*. Taken together, these data demonstrated that CCL7 is the functional target of miR-23b.

LV-miR23b Amelioration of Disease Development Depends on the Inhibition of Leukocyte Migration

To confirm that miR-23b can directly inhibit leukocyte infiltration rather than modulate encephalitogenic T cell differentiation, we first used a transwell system to test cellular migration ability *in vitro*. Primary astrocytes, which can secrete CCL7 when stimulated with lipopolysaccharide (LPS), were seeded in the lower level of transwells in the presence or absence of LPS for 18 hr. Then, dLN cells were obtained from LV-Ctrl-treated and LV-miR23b-treated EAE mice, cultured for 3 hr in the upper level of transwells, and the percentage of migrating dLN cells was calculated. We observed that dLN cells from LV-miR23b-treated mice presented a similar migratory ability as those from LV-Ctrl-treated mice (Figure 5A), indicating that downregulation of miR-23b in dLN cells did not interfere with cellular migration when its functional target CCL7 was present and sufficient. Next, we cultured dLN cells from EAE mice for 3 hr in the upper level of a transwell, and we seeded primary astrocytes in the lower level as was previously done, while stimulating them with LPS before adding LV-Ctrl or LV-miR23b. We found that adding miR-23b in culture medium significantly inhibited CCL7 production of astrocytes (Figure 5B) and reduced the migration of draining lymphocytes (Figure 5C). Similar to LV-miR23b, CCL7-neutralizing antibody also markedly prevented the migration of MOG-primed lymph node cells toward LPS-stimulated astrocytes (Figure 5D). Conversely, the inhibited lymphocyte migration by LV-miR23b was almost completely rescued by the addition of rmCCL7 (Figure 5D). These results, together, suggested that supplying miR-23b directly interferes with dLN cell migration by targeting the CCL7 production of astrocytes.

To further confirm whether miR-23b directly affects the encephalitogenesis of effector $CD4^+$ T cells, splenocytes from the LV-miR23b- or LV-Ctrl-treated EAE mice were restimulated with MOG_{35-55} for 3 days; $CD4^+$ T cells from different groups were then isolated and transferred into naive wild-type (WT) mice. The results showed that there was no obvious difference between these two groups (Figure 5E). In another experiment, on day 10 p.i., splenocytes from EAE mice were restimulated with MOG_{35-55} and IL-23 for

3 days to induce Th17 cells; $CD4^+$ T cells were then isolated and transferred into naive WT mice, which were treated with LV-Ctrl or LV-miR23b 3 days later. The results showed that recipient mice treated with LV-miR23b developed an obviously milder clinical disease compared with LV-Ctrl-treated mice (Figure 5F). These data confirmed that LV-miR23b ameliorates disease severity by inhibiting the migration of pathogenic T cells to the CNS, rather than directly diminishing the encephalitogenesis of effector $CD4^+$ T cells.

DISCUSSION

Several unique miRNAs have been found to be specifically expressed in MS patients, but the underlying mechanism of miRNAs in regulation of the pathogenesis of MS is still unclear. In this study, we show that overexpression of miR-23b *in vivo* has a beneficial effect on EAE, an animal model of MS, by impairing encephalitogenic Th1 and Th17 cell infiltration into the CNS. Importantly, our studies identified CCL7 as the functional target of miR-23b. Together, our data show a novel mechanism of action exerted by miR-23b, the inhibition of cell migration rather than modulation of the specific inflammatory response. These findings are interesting and shed light on a possible therapeutic potential of miR-23b in the treatment of MS.

Acute MS is characterized by extensive infiltration of inflammatory cells in the CNS, where they promote tissue damage and axonal death.[1,23,24] Therapies focused on immunomodulation and cellular infiltration in the CNS are, therefore, of great importance. We observed that overexpression of miR-23b starting on the day of immunization resulted in a mild form of EAE and did not impair the subpopulations of encephalitogenic T cells in the periphery. This is interesting as the migratory ability of leukocytes to the sites of inflammation was reduced in the miR-23b-treated EAE mice. Since there is no evidence of the effect of miR-23b on T cell migration and EAE prevention, our results characterize a previously unknown miR-23b function in leukocyte migration, and they open new perspectives for the use of miRNAs to treat relapse of MS and other autoimmune diseases.

Numerous studies have shown that miR-23b is involved in cell metabolism and cancer development,[25–28] which led us to find additional mechanisms in MS. Here we explored the possibility that miR-23b may act as an inhibitor of chemoattractants for leukocytes. To test this hypothesis, we measured the ability of miR-23b in *in vitro* and *in vivo* experiments. The results demonstrated that miR-23b inhibits the chemotaxis of leukocytes. An *in vivo* disease model of EAE revealed that overexpression of miR-23b reduced the numbers of leukocytes infiltrated into the CNS and alleviated disease symptoms. These results suggest that leukocyte migration to the sites of inflammation may be influenced by miR-23b.

Recently, accumulating evidence suggests that miR-23b plays an important role in autoimmune pathogenesis, which led us to attempt to determine the underlying mechanism. Zhu et al.[25] showed that miR-23b targets TAB2, TAB3, and IKK-α and suppresses nuclear factor κB (NF-κB) activation in animal lupus, rheumatoid arthritis, and MS. In addition, Wu et al.[29] demonstrated that the expression levels of NF-κB, tumor necrosis factor alpha (TNF-α), IL-6, and ICAM-1 were decreased after transfected with miR-23b mimics in vascular endothelial cells, and they indicated that miR-23b may play a significant role in the pathogenesis and progression of sepsis. However, the above studies mainly focused on the relationship between miR-23b and the NF-κB-signaling pathway, and, therefore, they did not study the effect of miR-23b on cell migration. Here we identified CCL7, a secreted chemokine that attracts monocytes during inflammation and metastasis,[23,30,31] as a novel target of miR-23b.

Interaction of chemokines and their receptors mediates a variety of leukocyte responses, including immune activation and chemotaxis.[32] White matter lesions in the CNS of acute EAE and MS patients demonstrate high levels of CCL2, CCL3, CCL4, CCL5, and CCL7, chemokines that are involved in the accumulation and activation of leukocytes bearing CCR2, CCR4, CCR5, and CCR6 receptors.[21,33–35] Previous studies showed that chemokine CCL7 acts as a CCR2 ligand, attracts monocytes,[23] and regulates macrophage function.[30] There is also evidence showing that CCR2 is expressed on T cell lineages, especially Th17 cells.[31,36] Additionally, accumulating evidence raises the possibility that CCR2 on Th17 cells may be a therapeutic target in MS.[35,37–39] Our data therefore suggest that miR-23b regulates T cell migration in EAE development, and they demonstrate that CCL7, commonly secreted by astrocytes, is specifically targeted by miR-23b, which reduces cell infiltration to the CNS.[21,29]

Our results demonstrated that miR-23b treatment did not completely block inflammatory cell migration. One possible reason is that different tissues and organs express several chemokines that attract certain immune cells.[3] Astrocytes, the major group of glial cells in the CNS, affect many aspects of inflammation and immune reactivity within the brain and spinal cord. Activated astrocytes produce chemokines like CCL2, CCL7, and CXCL1, etc.[21] Although CCR2 is expressed on T cells and, in particular, on Th17 cells, their migration is also probably affected by other chemokine receptors, like CCR4, CCR6, etc.[33] miR-23b may thus partially prevent Th17 migration and alleviate disease development.

Recent studies have suggested that miR-23b may play an immunomodulatory role in other types of immune cells, including monocytes, macrophages, and dendritic cells (DCs). For instance, miR-23b has been found to be expressed on tolerogenic human DCs and type 2 (M2) monocyte/macrophages.[40,41] miR-23b inhibits IL-12 production in human monocyte/macrophages,[42] and it plays an essential role in the inhibitory effect of bone marrow mesenchymal stem cells on DC differentiation and maturation.[43] While we in the present study focused on the effect of miR-23b on T cell responses in the development of EAE, the function of miR-23b on other immune cells and in EAE development requires further investigation.

In summary, our results characterize a novel aspect of miR-23b function in leukocyte migration, and they identify miR-23b as a

potential therapeutic target in the amelioration of MS and likely other autoimmune diseases.

MATERIALS AND METHODS

Mice and EAE Induction

WT female C57BL/6 mice were purchased from the Fourth Military University (Xi'an, China). All experimental procedures and protocols were approved by the Institutional Animal Care and Use committee of Shaanxi Normal University, and they were carried out in accordance with the approved institutional guidelines and regulations. Mice were maintained under standard conditions (23°C ± 2°C) in the Shaanxi Normal University Animal Facility. Mice were immunized at two sites on the back with 200 μg MOG_{35-55} (Genescript, Piscataway, NJ) in 200 μL emulsion containing 50% complete Freund's adjuvant with 5 mg/mL Mycobacterium tuberculosis H37Ra (Difco Laboratories, Lawrence, KS). All mice were intraperitoneally (i.p.) injected with 200 ng pertussis toxin (Sigma-Aldrich) in PBS on days 0 and 2 p.i. Clinical EAE was scored daily in a blind manner, according to a 0–5 scale as described previously: 0, no clinical signs; 0.5, stiff tail; 1, limp tail; 1.5, limp tail and waddling gait; 2, paralysis of one limb; 2.5, paralysis of one limb and weakness of another limb; 3, complete paralysis of both hind limbs; 4, moribund; and 5, death.[44] Cumulative clinical scores of each mouse were calculated by adding scores of the mouse from day 0 to day 40 p.i.

Construction of Vectors Expressing miR-23b and Dual Direction Fluorescence Reporter

Lentiviral vector backbone plasmid pCDH-CMV-MCS-EF1-copGFP was digested with XbaI and SalI to remove multiple cloning sites, EF1 promoter, and copGFP. The GFP open reading frame (ORF) fragment was amplified by primer pair GFPF and GFPR and cloned into downstream of CMV promoter, after which a 100-bp genomic sequence spanning the mouse miR-23b coding region and the flanking region from 5′ or 3′ on either end was cloned into the downstream of the GFP gene to form a pLV-miR23b lentiviral vector. Primer sequences are listed in Table S1. Positive clones were screened by enzyme digestion and DNA sequence. The vector that was inserted with a random sequence of miRNA was used as a vector control. Virus was produced according to the manual of Lenti-X HTX Packaging system (Clontech Laboratories, Mountain View, CA). For direct *in vivo* injection, approximately 2×10^7 transforming units of recombinant lentivirus were injected through the tail vein into each mouse.

A controllable dual-direction fluorescence reporter vector was modified based on the plasmid of pTRE3G-BI-mCherry (Clontech Laboratories, Mountain View, CA). Briefly, the copGFP was inserted into the C terminus of $P_{TRE3G-BI}$ and mCherry was located at the N terminus of $P_{TRE3G-BI}$. Meanwhile, the 3′ UTR of CCL7 was inserted into the 3′ of mCherry. The positive clones were screened by enzyme digestion and DNA sequence. For plasmid transfection, 500 ng pTRE3G-BI-copGFP/mCherry-CCL7UTR and control vector pTRE3G-BI-copGFP/mCherry were transfected to 293 cells separately. 1.5 μg/mL doxycycline (Dox) was added to activate the promoter of TRE3G.[45]

Histological Analysis

Mice were sacrificed at different time points after treatment and transcardially perfused with PBS. Brain and lumbar spinal cords were harvested for pathological assessment and spleen for immunological assessment. CNS tissues were cut into 5-μm sections, fixed with 4% paraformaldehyde, and stained with H&E for assessment of inflammation and Luxol fast blue (LFB) for demyelination. Slides were assessed and scored in a blinded fashion for inflammation as follows: 0, none; 1, a few inflammatory cells; 2, organization of perivascular infiltrates; and 3, abundant perivascular cuffing with extension into the adjacent tissue.[45] For demyelination quantification, total white matter was manually outlined, and area (%) of demyelination was calculated by Image-Pro Plus software.[44]

For immunohistochemistry, brain and spinal cord tissues were fixed using 4% paraformaldehyde for 1 day and then cryo-protected using 30% sucrose solution for 3 days. Fixed tissues were embedded in OCT compound (Tissue-Tek, Sakura Finetek, Japan) for frozen sections and then sectioned coronally at 12 μm. Transverse sections of brain and spinal cord were cut and stained with different antibodies. Immunofluorescence controls were routinely generated by omitting primary antibodies. Results were visualized by fluorescent microscopy (Nikon Eclipse E600; Nikon, Melville, NY) or confocal microscopy (Zeiss LSM 510; Carl Zeiss, Thornwood, NY). For the quantifications of H&E, LFB, and $CD45^+$, ten areas in the white matter of the lumbar spinal cord were selected, following a previous description.[44]

MNC Preparation

Spleen was mechanically dissociated through a 70-μm cell strainer (Falcon, Tewksbury, MA) and incubated with red blood cell lysis buffer (BioLegend, San Diego, CA) for 1 min. Harvested cells were washed with cold PBS before *in vitro* stimulation. To acquire CNS cells, spinal cords and brains were mechanically dissociated and incubated with Liberase (Roche, Nutley, NJ) for 30 min, passed through a 70-μm cell strainer, and washed with cold PBS. Cells were then fractionated on a 70%/30% Percoll (Sigma-Aldrich) gradient by centrifugation at 2,000 rpm for 20 min, and MNCs were collected from the interface and washed with PBS.

Flow Cytometry Analysis

For surface-marker staining, cells were incubated with fluorochrome-conjugated antibodies (Abs) to CD4 and CD8 (BD Biosciences, San Jose, CA) or isotype control Abs for 30 min on ice. For intracellular staining, splenocytes or CNS-infiltrating MNCs were stimulated with 25 and 10 μg/mL MOG peptide for 72 hr or overnight, respectively, followed by stimulation with 50 ng/mL phorbol 12-myristate 13-acetate (PMA) and 500 ng/mL ionomycin in the presence of GolgiPlug for 5 hr. Cells were surface stained with monoclonal antibodies (mAbs) against CD4 and CD8. Cells were then washed, fixed, and permeabilized with FIX&PERM solution (Invitrogen,

Gaithersburg, MD), and intracellular cytokines were stained with Abs against IL-17, IFN-γ, or GM-CSF (BD Biosciences). Flow cytometry analysis was performed on FACSAria (BD Biosciences), and data were analyzed with FlowJo software (Tree Star, Ashland, OR).

Real-Time PCR

Total RNA was extracted from cells or tissues using RNeasy Plus Mini Kit (QIAGEN, Valencia, CA) according to the manufacturer's instructions. Reverse transcription was conducted using QuantiTect Reverse Transcription Kit (QIAGEN). Real-time PCR was performed using the QuantiFast SYBR Green PCR Kit (QIAGEN), and detection was performed using the ABI Prism 7500 Sequence Detection System (Applied Biosystems, Foster City, CA). Glyceraldehyde 3-phosphate dehydrogenase (GAPDH) was used as an internal control. Neucleotide sequences of the primers were based on published cDNA sequences (Table S2).

Isolation of Astrocytes from the CNS of Adult Mice

Astrocytes were isolated from the CNS as previously described[46,47] with minor modifications. Naive and EAE mice were euthanatized, and then they were subjected to perfusion through the left ventricle with sterile PBS. Spinal cord and brains were removed, minced, and dissociated by neural tissue dissociation kits (Miltenyi Biotec, San Diego, CA) following the protocol. The digested tissue was passed through a 100-Mm cell strainer. Cells were then fractionated on a 70%/30% Percoll (Sigma-Aldrich) gradient by centrifugation at 2,000 rpm at 4°C for 20 min. Cells were collected from the 70%–30% interphase and then purified with anti-astrocyte cell surface antigen-2 (ACSA-2) microbeads (Miltenyi Biotec). Finally, the GFP+ astrocytes were sorted by FACSAria (BD Biosciences). To confirm that we had isolated a relatively pure population of GFP+ astrocytes, qPCR was performed for the astrocyte markers gfap, aldh111, and aqp4.

Migration Assays

Determination of the cellular migration ability was performed in a 24-well plate with transwell insert (pore size = 5 μm) (Corning Life Science, Pittston, PA). The migration method was followed as previously described.[24] In brief, 5×10^5 cells from dLNs were seeded in the upper level at a final volume of 100 μL in IMDM supplemented with 10% fetal bovine serum (FBS). The lower level was seeded with the astrocytes and filled with 500 μL medium in the absence or presence of anti-CCL7 or rmCCL7 (R&D Systems, Minneapolis, MN). As controls, some cells in the lower level received only medium. The lentivirus-treated groups were infected 3 days before adding LPS. The upper level cells were added to the transwell for 3 hr at 37°C. At the end of culture time, the cells in the lower level were counted by hemocytometer.

Western Blot Analysis

Brain and spinal cord tissues were harvested and homogenized, lysed with 2× Laemmli lysis buffer, and boiled at 100°C for 10 min. The lysates were then separated on 12% SDS-PAGE gels and transferred onto polyvinylidene fluoride (PVDF) membranes.[48] The membranes were immunoblotted with anti-MCP3 antibody (1:5,000, Abcam, Cambridge, MA), followed by incubation with horseradish peroxidase-conjugated secondary antibodies (1:10,000; Abcam), and finally developed with enhanced chemiluminescent (ECL; Thermo Scientific) substrates. Densitometry analysis of blotting images was done by using the quantificational method in ImageJ.

Cytokine Measurement by ELISA

Astrocytes were cultured at 2.0×10^6 cells/mL in DMEM supplemented with 10% FBS in 24-well plates and stimulated with LPS for 24 hr. Supernatants were harvested and assayed for CCL7 using ELISA kits (R&D Systems). The optical density was determined by Multiskan FC microplate photometer (Thermo Fisher Scientific) at 450 nm.

Statistical Analysis

Statistical analyses were performed using GraphPad Prism 6 software (GraphPad, La Jolla, CA). Data are presented as mean ± SD. When comparing multiple groups, data were analyzed by ANOVA with Tukey's multiple comparisons test. A significance criterion of $p < 0.05$ was used for all statistical analysis.

SUPPLEMENTAL INFORMATION

Supplemental Information includes three figures and two tables and can be found with this article online at https://doi.org/10.1016/j.ymthe.2017.11.013.

AUTHOR CONTRIBUTIONS

Y.Z. and X.L. conceived and designed the experiments, analyzed data, and wrote the manuscript. Y.Z., X.-Y.L., J.-J.H., L.Z., and F.Z. carried out the experiments. J.R. performed the flow cytometry experiment. Z.-Z.W. and G.-X.Z. co-supervised the study and wrote the paper. All authors read and approved the final manuscript.

CONFLICTS OF INTEREST

None of the authors have a conflict of interest.

ACKNOWLEDGMENTS

This study was supported by the Chinese National Natural Science Foundation (grants 81501062 and 81771345) and the Fundamental Research Funds for the Central Universities (grants GK201603114, GK201703079, GK201701009, 2017CSY021, and 2017CSZ007). We thank Katherine Regan for editorial assistance.

REFERENCES

1. Yang, J., Yan, Y., Ciric, B., Yu, S., Guan, Y., Xu, H., Rostami, A., and Zhang, G.X. (2010). Evaluation of bone marrow- and brain-derived neural stem cells in therapy of central nervous system autoimmunity. Am. J. Pathol. *177*, 1989–2001.

2. Mandolesi, G., Gentile, A., Musella, A., Fresegna, D., De Vito, F., Bullitta, S., Sepman, H., Marfia, G.A., and Centonze, D. (2015). Synaptopathy connects inflammation and neurodegeneration in multiple sclerosis. Nat. Rev. Neurol. *11*, 711–724.

3. Lee, W., Su Kim, H., and Lee, G.R. (2015). Leukotrienes induce the migration of Th17 cells. Immunol. Cell Biol. *93*, 472–479.

4. Zhang, Y., Li, X., Ciric, B., Ma, C.G., Gran, B., Rostami, A., and Zhang, G.X. (2015). Therapeutic effect of baicalin on experimental autoimmune encephalomyelitis is mediated by SOCS3 regulatory pathway. Sci. Rep. *5*, 17407.
5. El-Behi, M., Ciric, B., Dai, H., Yan, Y., Cullimore, M., Safavi, F., Zhang, G.X., Dittel, B.N., and Rostami, A. (2011). The encephalitogenicity of T(H)17 cells is dependent on IL-1- and IL-23-induced production of the cytokine GM-CSF. Nat. Immunol. *12*, 568–575.
6. Garo, L.P., and Murugaiyan, G. (2016). Contribution of MicroRNAs to autoimmune diseases. Cell. Mol. Life Sci. *73*, 2041–2051.
7. Guan, H., Fan, D., Mrelashvili, D., Hao, H., Singh, N.P., Singh, U.P., Nagarkatti, P.S., and Nagarkatti, M. (2013). MicroRNA let-7e is associated with the pathogenesis of experimental autoimmune encephalomyelitis. Eur. J. Immunol. *43*, 104–114.
8. O'Connell, R.M., Rao, D.S., and Baltimore, D. (2012). microRNA regulation of inflammatory responses. Annu. Rev. Immunol. *30*, 295–312.
9. Isaacs, S.R., Wang, J., Kim, K.W., Yin, C., Zhou, L., Mi, Q.S., and Craig, M.E. (2016). MicroRNAs in Type 1 Diabetes: Complex Interregulation of the Immune System, β Cell Function and Viral Infections. Curr. Diab. Rep. *16*, 133.
10. Salehi, E., Eftekhari, R., Oraei, M., Gharib, A., and Bidad, K. (2015). MicroRNAs in rheumatoid arthritis. Clin. Rheumatol. *34*, 615–628.
11. Shen, N., Liang, D., Tang, Y., de Vries, N., and Tak, P.P. (2012). MicroRNAs–novel regulators of systemic lupus erythematosus pathogenesis. Nat. Rev. Rheumatol. *8*, 701–709.
12. Simpson, L.J., Patel, S., Bhakta, N.R., Choy, D.F., Brightbill, H.D., Ren, X., Wang, Y., Pua, H.H., Baumjohann, D., Montoya, M.M., et al. (2014). A microRNA upregulated in asthma airway T cells promotes TH2 cytokine production. 15, 1162–1170.
13. Junker, A., Hohlfeld, R., and Meinl, E. (2011). The emerging role of microRNAs in multiple sclerosis. Nat. Rev. Neurol. *7*, 56–59.
14. Thamilarasan, M., Koczan, D., Hecker, M., Paap, B., and Zettl, U.K. (2012). MicroRNAs in multiple sclerosis and experimental autoimmune encephalomyelitis. Autoimmun. Rev. *11*, 174–179.
15. Zhu, E., Wang, X., Zheng, B., Wang, Q., Hao, J., Chen, S., Zhao, Q., Zhao, L., Wu, Z., and Yin, Z. (2014). miR-20b suppresses Th17 differentiation and the pathogenesis of experimental autoimmune encephalomyelitis by targeting RORγt and STAT3. J. Immunol. *192*, 5599–5609.
16. O'Connell, R.M., Kahn, D., Gibson, W.S., Round, J.L., Scholz, R.L., Chaudhuri, A.A., Kahn, M.E., Rao, D.S., and Baltimore, D. (2010). MicroRNA-155 promotes autoimmune inflammation by enhancing inflammatory T cell development. Immunity *33*, 607–619.
17. Murugaiyan, G., Beynon, V., Mittal, A., Joller, N., and Weiner, H.L. (2011). Silencing microRNA-155 ameliorates experimental autoimmune encephalomyelitis. J. Immunol. *187*, 2213–2221.
18. Du, C., Liu, C., Kang, J., Zhao, G., Ye, Z., Huang, S., Li, Z., Wu, Z., and Pei, G. (2009). MicroRNA miR-326 regulates TH-17 differentiation and is associated with the pathogenesis of multiple sclerosis. Nat. Immunol. *10*, 1252–1259.
19. Mycko, M.P., Cichalewska, M., Machlanska, A., Cwiklinska, H., Mariasiewicz, M., and Selmaj, K.W. (2012). MicroRNA-301a regulation of a T-helper 17 immune response controls autoimmune demyelination. Proc. Natl. Acad. Sci. USA *109*, E1248–E1257.
20. Zamvil, S.S., and Steinman, L. (1990). The T lymphocyte in experimental allergic encephalomyelitis. Annu. Rev. Immunol. *8*, 579–621.
21. Jiang, B.C., Cao, D.L., Zhang, X., Zhang, Z.J., He, L.N., Li, C.H., Zhang, W.W., Wu, X.B., Berta, T., Ji, R.R., and Gao, Y.J. (2016). CXCL13 drives spinal astrocyte activation and neuropathic pain via CXCR5. J. Clin. Invest. *126*, 745–761.
22. Renner, N.A., Ivey, N.S., Redmann, R.K., Lackner, A.A., and MacLean, A.G. (2011). MCP-3/CCL7 production by astrocytes: implications for SIV neuroinvasion and AIDS encephalitis. J. Neurovirol. *17*, 146–152.
23. Xuan, W., Qu, Q., Zheng, B., Xiong, S., and Fan, G.H. (2015). The chemotaxis of M1 and M2 macrophages is regulated by different chemokines. J. Leukoc. Biol. *97*, 61–69.
24. Thomé, R., de Carvalho, A.C., Alves da Costa, T., Ishikawa, L.L., Fraga-Silva, T.F., Sartori, A., de Oliveira, A.L., and Verinaud, L. (2016). Artesunate Ameliorates Experimental Autoimmune Encephalomyelitis by Inhibiting Leukocyte Migration to the Central Nervous System. CNS Neurosci. Ther. *22*, 707–714.
25. Zhu, S., Pan, W., Song, X., Liu, Y., Shao, X., Tang, Y., Liang, D., He, D., Wang, H., Liu, W., et al. (2012). The microRNA miR-23b suppresses IL-17-associated autoimmune inflammation by targeting TAB2, TAB3 and IKK-α. Nat. Med. *18*, 1077–1086.
26. Wang, P., Zhang, J., Zhang, L., Zhu, Z., Fan, J., Chen, L., Zhuang, L., Luo, J., Chen, H., Liu, L., et al. (2013). MicroRNA 23b regulates autophagy associated with radioresistance of pancreatic cancer cells. Gastroenterology *145*, 1133–1143.e12.
27. Gao, P., Tchernyshyov, I., Chang, T.C., Lee, Y.S., Kita, K., Ochi, T., Zeller, K.I., De Marzo, A.M., Van Eyk, J.E., Mendell, J.T., and Dang, C.V. (2009). c-Myc suppression of miR-23a/b enhances mitochondrial glutaminase expression and glutamine metabolism. Nature *458*, 762–765.
28. Zhang, H., Hao, Y., Yang, J., Zhou, Y., Li, J., Yin, S., Sun, C., Ma, M., Huang, Y., and Xi, J.J. (2011). Genome-wide functional screening of miR-23b as a pleiotropic modulator suppressing cancer metastasis. Nat. Commun. *2*, 554.
29. Wu, M., Gu, J.T., Yi, B., Tang, Z.Z., and Tao, G.C. (2015). microRNA-23b regulates the expression of inflammatory factors in vascular endothelial cells during sepsis. Exp. Ther. Med. *9*, 1125–1132.
30. Lim, H.W., Lee, J., Hillsamer, P., and Kim, C.H. (2008). Human Th17 cells share major trafficking receptors with both polarized effector T cells and FOXP3+ regulatory T cells. J. Immunol. *180*, 122–129.
31. Bromley, S.K., Mempel, T.R., and Luster, A.D. (2008). Orchestrating the orchestrators: chemokines in control of T cell traffic. Nat. Immunol. *9*, 970–980.
32. Holman, D.W., Klein, R.S., and Ransohoff, R.M. (2011). The blood-brain barrier, chemokines and multiple sclerosis. Biochim. Biophys. Acta *1812*, 220–230.
33. Cheng, W.J., and Chen, G.J. (2014). Chemokines and Chemokine Receptors in Multiple Sclerosis (Mediat Inflamm).
34. Yang, J., Yan, Y., Ma, C.G., Kang, T., Zhang, N., Gran, B., Xu, H., Li, K., Ciric, B., Zangaladze, A., et al. (2012). Accelerated and enhanced effect of CCR5-transduced bone marrow neural stem cells on autoimmune encephalomyelitis. Acta Neuropathol. *124*, 491–503.
35. Kara, E.E., McKenzie, D.R., Bastow, C.R., Gregor, C.E., Fenix, K.A., Ogunniyi, A.D., Paton, J.C., Mack, M., Pombal, D.R., Seillet, C., et al. (2015). CCR2 defines in vivo development and homing of IL-23-driven GM-CSF-producing Th17 cells. Nat. Commun. *6*, 8644.
36. Eltayeb, S., Berg, A.L., Lassmann, H., Wallström, E., Nilsson, M., Olsson, T., Ericsson-Dahlstrand, A., and Sunnemark, D. (2007). Temporal expression and cellular origin of CC chemokine receptors CCR1, CCR2 and CCR5 in the central nervous system: insight into mechanisms of MOG-induced EAE. J. Neuroinflammation *4*, 14.
37. Aranami, T., and Yamamura, T. (2008). Th17 Cells and autoimmune encephalomyelitis (EAE/MS). Allergol. Int. *57*, 115–120.
38. Gaupp, S., Pitt, D., Kuziel, W.A., Cannella, B., and Raine, C.S. (2003). Experimental autoimmune encephalomyelitis (EAE) in CCR2(-/-) mice: susceptibility in multiple strains. Am. J. Pathol. *162*, 139–150.
39. Lindner, M., Thümmler, K., Arthur, A., Brunner, S., Elliott, C., McElroy, D., Mohan, H., Williams, A., Edgar, J.M., Schuh, C., et al. (2015). Fibroblast growth factor signalling in multiple sclerosis: inhibition of myelination and induction of pro-inflammatory environment by FGF9. Brain *138*, 1875–1893.
40. Stumpfova, Z., Hezova, R., Meli, A.C., Slaby, O., and Michalek, J. (2014). MicroRNA profiling of activated and tolerogenic human dendritic cells. Mediators Inflamm. *2014*, 259689.
41. Lu, L., McCurdy, S., Huang, S., Zhu, X., Peplowska, K., Tiirikainen, M., Boisvert, W.A., and Garmire, L.X. (2016). Time Series miRNA-mRNA integrated analysis reveals critical miRNAs and targets in macrophage polarization. Sci. Rep. *6*, 37446.
42. Cui, B., Liu, W., Wang, X., Chen, Y., Du, Q., Zhao, X., Zhang, H., Liu, S.L., Tong, D., and Huang, Y. (2017). Brucella Omp25 Upregulates miR-155, miR-21-5p, and miR-23b to Inhibit Interleukin-12 Production via Modulation of Programmed Death-1 Signaling in Human Monocyte/Macrophages. Front. Immunol. *8*, 708.
43. Wu, J., Ji, C., Cao, F., Lui, H., Xia, B., and Wang, L. (2017). Bone marrow mesenchymal stem cells inhibit dendritic cells differentiation and maturation by microRNA-23b. Biosci. Rep. *37*, BSR20160436.

44. Li, X., Zhang, Y., Yan, Y., Ciric, B., Ma, C.G., Gran, B., Curtis, M., Rostami, A., and Zhang, G.X. (2016). Neural Stem Cells Engineered to Express Three Therapeutic Factors Mediate Recovery from Chronic Stage CNS Autoimmunity. Mol. Ther. *24*, 1456–1469.

45. Li, X., Zhang, Y., Yan, Y., Ciric, B., Ma, C.G., Chin, J., Curtis, M., Rostami, A., and Zhang, G.X. (2017). LINGO-1-Fc-Transduced Neural Stem Cells Are Effective Therapy for Chronic Stage Experimental Autoimmune Encephalomyelitis. Mol. Neurobiol. *54*, 4365–4378.

46. Mayo, L., Trauger, S.A., Blain, M., Nadeau, M., Patel, B., Alvarez, J.I., Mascanfroni, I.D., Yeste, A., Kivisäkk, P., Kallas, K., et al. (2014). Regulation of astrocyte activation by glycolipids drives chronic CNS inflammation. Nat. Med. *20*, 1147–1156.

47. Rothhammer, V., Mascanfroni, I.D., Bunse, L., Takenaka, M.C., Kenison, J.E., Mato, L., Chao, C.C., Patel, B., Yan, R., Blain, M., et al. (2016). Type I interferons and microbial metabolites of tryptophan modulate astrocyte activity and central nervous system inflammation via the aryl hydrocarbon receptor. Nat. Med. *22*, 586–597.

48. Zhang, Y., Li, X., Ciric, B., Ma, C.G., Gran, B., Rostami, A., and Zhang, G.X. (2017). Effect of Fingolimod on Neural Stem Cells: A Novel Mechanism and Broadened Application for Neural Repair. Mol. Ther. *25*, 401–415.

YMTHE, Volume *26*

Supplemental Information

miR-23b Suppresses Leukocyte Migration and Pathogenesis of Experimental Autoimmune Encephalomyelitis by Targeting CCL7

Yuan Zhang, Juan-Juan Han, Xiao-Yan Liang, Li Zhao, Fei Zhang, Javad Rasouli, Zhe-Zhi Wang, Guang-Xian Zhang, and Xing Li

Supplementary Figure1

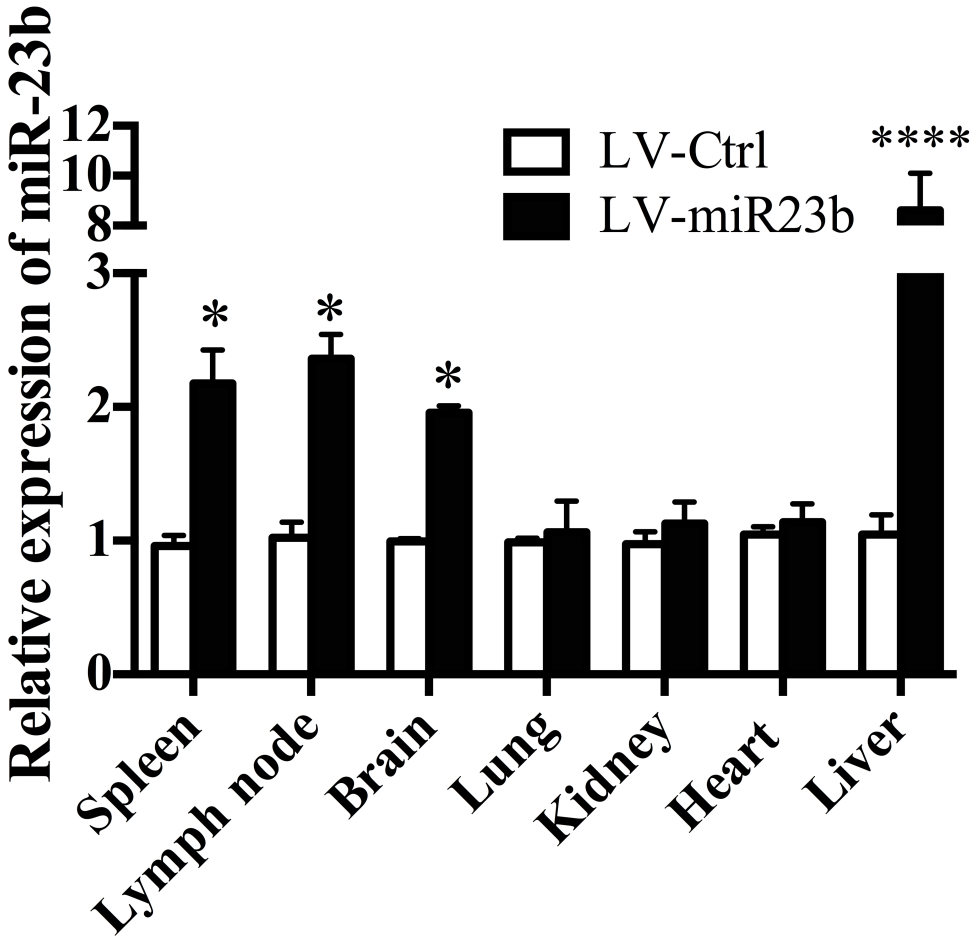

Supplementary Figure 1. qPCR analysis of miR-23b expression from spleen, lymph node, brain, lung, kidney, heart and liver of mice infected with LV-Ctrl and LV-miR23b after 5 d. Fold change are normalized to the average of LV-Ctrl-infected mice are presented relative to RNU6B. Lentivirus infected mice, n = 3. * $p < 0.05$; **** $p < 0.0001$.

Supplementary Figure2

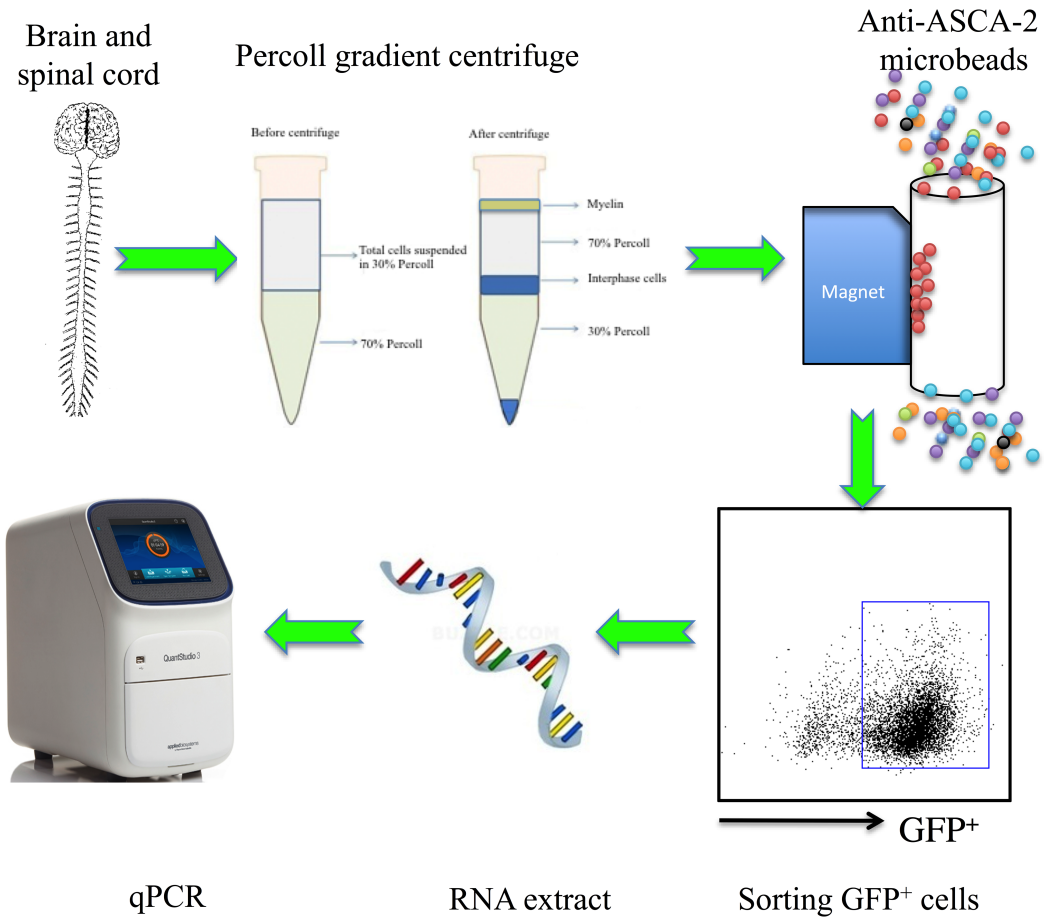

Supplenmentary Figure 2. Flow chart of determines the CCL7 expression level from GFP^+ astrocytes.

Supplementary Figure3

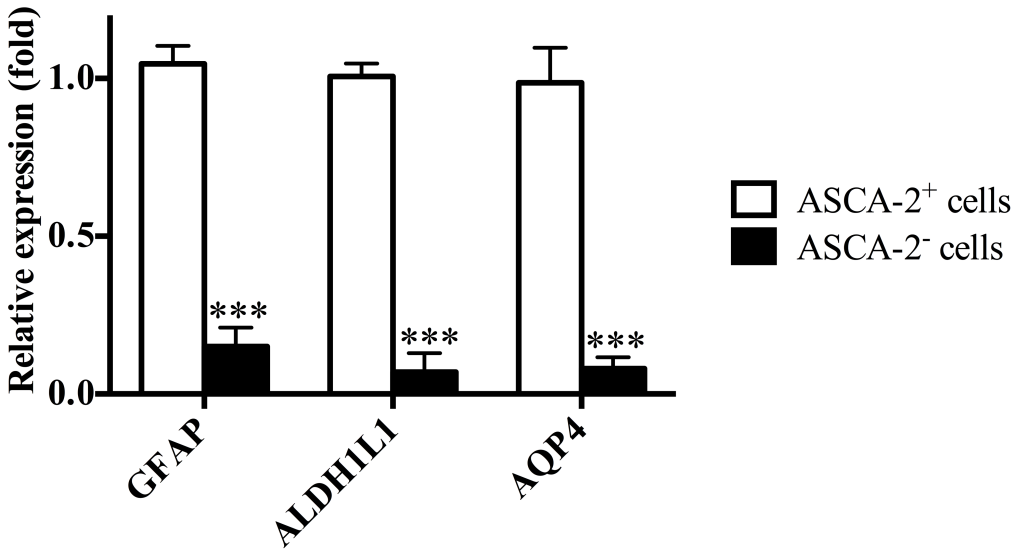

Supplementary Figure 3. qPCR analysis of astrocytes isolated from brain and spinal cord tissue by anti-ASCA-2 microbeads. Data are ± SD (n=3) (Two-way ANOVA). ***p< 0.001.

Table S1. Primers used for pTRE3G-BI-copGFP/mCherry-CCL7UTR vector construction

Primer name	Sequences (5'-3')
GFP SalI F:	ACT GTC GAC ATG GAG AGC GAC GAG AGC GG
GFP BglII R:	CTT ATA GCT TTA GCG AGA TCC GGT GGA GC
mCherry EcoRI F:	ACT GAA TTC ATG GTG AGC AAG GGC GAG GA
mCherry XbaI R:	CTT TCT AGA TGG ACG AGC TGT ACA AGT AA
mCCL7 3'UTR BamHI F	ACT GGA TCC TGCCTGAACAGAAACCAACC
mCCL7 3'UTR NotI R	CTT GCG GCC GCT GAT TCT TGC AAA GTC CCT TCA

Table S2.

Gene	Primers	
	Sense (5'-3')	Anti-sense (5'-3')
CCR2	GCCATCATAAAGGAGCCATACC	TGTGGTGAATCCAATGCCCT
CCR5	CTGCTGCCTAAACCCTGTCA	TGCAAAAGCGTTTGACCATGT
CCR6	GCCCTGGAAAGCTGGGTAAA	GGCAGACACTCACAGTACCC
CCR7	GGAAACCCAGGAAAAACGTGC	TCCTTCTTGAAGCACACCGA
CXCR3	ACAACTGAGGCCTCCTACCT	ATGCTGAGCTGTCAGTGCAT
CCL2	CAGGTCCCTGTCATGCTTCT	GTGGGGCGTTAACTGCATCT
CCL3	GCTTCTCCTACAGCCGGAAG	AGGTCTCTTTGGAGTCAGCG
CCL4	CCCAGCTCTGTGCAAACCTA	CCATTGGTGCTGAGAACCCT
CCL5	GTGCCCACGTCAAGGAGTAT	TTCTCTGGGTTGGCACACAC
CCL7	CGCTGCTTTCAGCATCCAAG	CTTCCCAGGGACACCGACTA
CCL8	TCTACGCAGTGCTTCTTTGC	AGCAGGTGACTGGAGCCTTA
CCL9	GCCCAGATCACACATGCAAC	AGGACAGGCAGCAATCTGAA
CCL11	AGAGCTCCACAGCGCTTCTA	GGAAGTTGGGATGGAGCCTG
CCL19	GAAGACTGCTGCCTGTCTGT	GCCCCTTAGTGTGGTGAACA
CCL20	AGCAGCAAGCAACTACGACT	TGGATCAGCGCACACAGATT